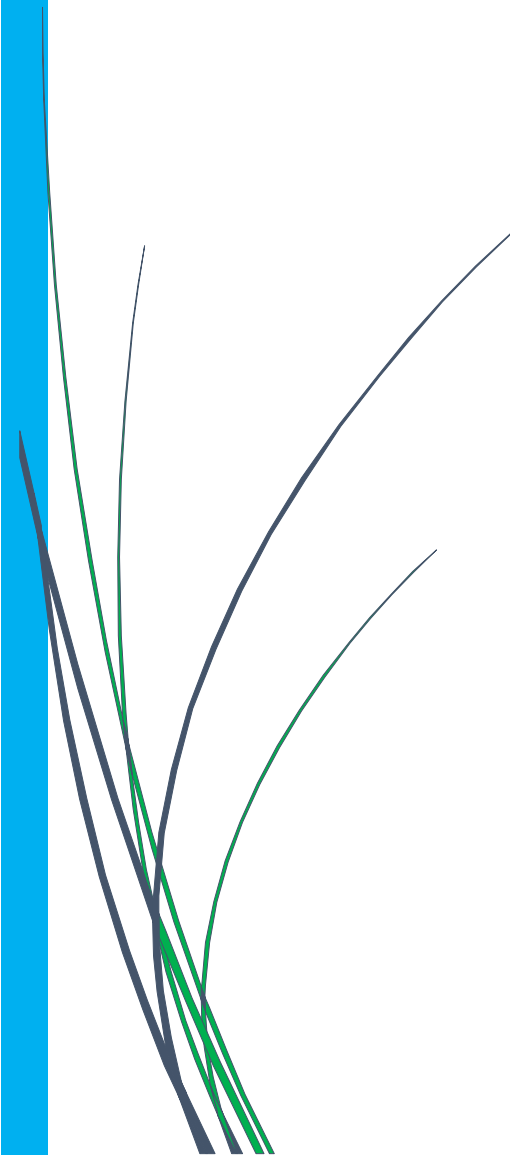# Chapter:1 Introduction and Literature Survey

1.1 Introduction

Global energy requirement is increasing, whereas, energy resources are depleting day by day. The renewable energy resources will be in demand not only in near future, but also a requisite for sustainable development and daily needs. Energy crisis, global warming, climate change and need for sustainable development have triggered global interest in developing renewable energy sources [1]. Under such a scenario, researchers look forward to hydrogen as a future energy for transportation, fuel cells and power stations [2-7]. The comparative study of technical and environmental issues between fossils fuels and hydrogen energy reveals hydrogen economy as an absolute solution for our planet from environmental challenges [8].

Hydrogen contains the highest energy content of any chemical fuel, but it is highly reactive gas and so is not found in a free state on earth. It is present in a compound form such as water, fossil hydrocarbon, biological constituent components (Carbohydrates cellulose, starch etc.), minerals (bicarbonate rocks), water etc. Hydrogen is secondary source of energy produced by conversion of primary source of energy. Hydrogen is the lightest gas with a density which is one fourteenth of the density of air and one ninth of the density of natural gas. Boiling point of hydrogen is 20K with a specific gravity of 0.07 which is roughly 1/10 of gasoline. The calorific value of natural gas is 38.3mJ/m^3, whereas the calorific value of hydrogen gas is 12.1mJ/m^3. Hydrogen is an ideal fuel. When hydrogen reacts with oxygen it forms water as a sole product and liberates energy:

$$H_2 + \frac{1}{2} O_2 \rightarrow H_2O + \text{Energy} \qquad (1.1)$$
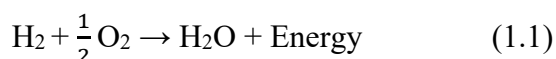
There are several attractive features of hydrogen which show its great feasibility among different available fuels in the future.

I. It can be produced from water abundantly available in nature.

II. It has the highest energy content/mass of any chemical fuel at present scenario.

III. It can be substituted for hydrocarbon in a broad range of applications.

IV. High combustion efficiency

V. Non-polluting and renewable resource.

VI. It can be used in fuel cell to produce electricity and useful heat.

Hydrogen flame speed is very high, so it is the best fuel for the rocket cryogenic engine which requires high thrust. Flameless oxidation of hydrogen on a catalyst surface at much lower temperature makes it the best fuel for fuel cell [7, 9].

1.2 Hydrogen in Indian prospects

India has a global identity as an agricultural economy. Now a days, due to unpredictable rains, seasonal variations provoke suicidal circumstances of farmers. This environmental problem is coming owing to anthropogenic intrusions in natural cycles for human benefit. However, the remedies are within environment in the form of fermenting microorganism which can ferment the crops and their residues into ethanol. Now, if we are looking for requirement of energy sources to meet the energy demands, ethanol production can reduce the dependency of India for energy over other countries. Economic prospects of the country will also be increased.

1.3 Current scenario of hydrogen generation

There are several pathways of hydrogen production, such as electrolysis, photolysis and thermolysis of water, biological reactions, gasification and pyrolysis of biomass, steam reforming and partial oxidation of hydrocarbons [10, 11]. Recently, photo-catalytic production of hydrogen from ethanol has also gained impetus [12, 13]. However, excessive requirement of electricity makes electrochemical process expensive and also, photolysis of water is highly expensive owing to requirement of expensive electrodes. Biological methods are also reported but they suffer from a lower rate of hydrogen generation. These drawbacks make thermo chemical method feasible pathway for hydrogen generation sustainably [14, 15]. All over the world, 50% feedstock of natural gases comprises hydrogen production via steam reforming which is not a renewable source [4]. Other feeds such as glycerol; methanol, and ethanol have also been used for the steam reforming to produce hydrogen. Among these ethanol steam reforming (ESR) using an appropriate catalyst shows the most efficient way of renewable hydrogen production[16] as represented by the following overall stoichiometric equation:

$$C_2H_5OH + 3H_2O \rightarrow 2CO_2 + 6H_2 \qquad (1.2)$$
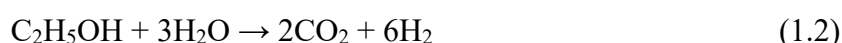
1.4 Literature survey for catalytic ESR reactions

Various types of catalysts such as noble metals (Pt, Pd, Rh, Au and Ru) [17-24], transition metals (Cu, Co and Ni) as well as the combinations of both [25-28] have been used to catalyse ESR reactions. However, these catalysts get deactivated due to carbonaceous deposits formed as the by-product during ESR reaction (described later under reaction mechanism). Up to 1990s, only a few papers discussed the catalytic steam reforming of ethanol [29-31], whereas, in the last two decades a lot of work has been done on modification strategies to minimize carbon formation during ESR.

In catalytic steam reforming of ethanol, noble metal catalysts show high activity and selectivity for hydrogen production with negligible or no coke formation [17, 18, 22, 28, 32-36]. However, noble metal catalysts are not cost effective [37]. In periodic table, among non-noble metal catalyst Cu, Ni and Co are reported to be most active metals for ESR[38]. Therefore, these metals have been widely studied on several supports such as Al_2O_3, SiO_2, ZrO_2 and CeO_2 [39]. Large volumes of research work have been reported on the deactivation of non-noble metal catalysts by carbonaceous deposition during ESR [40-46]. In this regard, the oxidative ESR on non-noble catalyst [47] is a good approach, though the carbonaceous deposition is comparatively lower than ESR, but the overall yield of hydrogen per mole of ethanol is also lower [48]. Modification of non-noble catalysts for high selectivity of desired gas is better way to produce hydrogen. The Table 1.1 summarized the different catalysts formulated to perform the ESR in literature.

The growth of carbon on the surface of catalyst is determined by the structure of hydrocarbons [49] (CH_4/ C_2H_6/C_2H_4) resulting as byproducts during ESR. Thus, the carbon source as well as catalyst composition play a major role in the rate of carbon deposition and its development. The rate of carbon deposition gets accelerated at high temperature [50]. The support as well as metal and support interface are the major sites for carbon deposition [51].

Table 1.1 The activity of different catalysts reported in literature for ESR

Catalyst		Reaction Condition		Ethanol	Hydrogen	Refer
Metal load (%)	Support	S/ E	Temp (K)	Conversion (%)	selectivity (%)	ences
Noble metals						
2 Rh	γ-Al_2O_3	3	1073	100	96	[52]
3 Rh	MgO	8.5	923	99	91	[53]
1 Rh	CeO_2	3	723	Above 90	82	[54]

2 Rh	CeO_2	8	723	100	69	[55]
2 Rh	ZrO_2	8	723	100	70.3	[56]
2 Rh	CeO_2- ZrO_2 (Ce/Zr = 1)	8	723	100	70.3	[57]
5 Ru	γ-Al_2O_3	3	1073	100	96	[52]
1Ru	CeO_2	3	723	Above 90	57	[55]
2.5Pt 1Ru	γ-Al_2O_3	10	823	100	100	[58]
1 Pt	γ-Al_2O_3	3	1073	100	96	[52]
0.5Pt	γ-Al_2O_3	4	613	95	40	[59]
1 Pt	CeO_2	3	573	100	39	[60]
1.5 Pt	CeO_2- ZrO_2 (Ce/Zr = 4)	10	823	100	88	[61]
1 Pd	γ-Al_2O_3	3	1073	55	50	[52]
5 Pd	γ-Al_2O_3	3	923	100	95	[62]
6Rh2Pt	La_2O_3	7	973	100	78	[63]
Ru	CeO_2/YSZ	5	853	100	86.6	[18]
Non noble metals						
7Ni	SiO_2	3.7	873	97.1	82.6	[64]
7Ni 10Ce				100	84.4	
7Ni 10Zr				100	82.5	
2Cu7Ni10 Mg	SiO_2	7.4	873	100	84.8	[40]
1Co	V_2O_5	13	723	100	53.5	[39]
	ZnO			100	71.3	
	La_2O_3			85	63.1	
	CeO_2			93.7	69.6	
	Sm_2O_3			85.9	64.7	
30ZnO	SiO_2	12	773	91.8	57.0	[65]
50ZnO	SiO_2			92.0	51.4	
70ZnO	SiO_2			92.3	61.0	
ZnO	-			91.7	58.6	
2Ir	CeO_2	3.2	923	100	75	[41]
2Ir	$Ce_{0.9}Pr_{0.1}O_2$	3	773	100	72	[66]
20Co	CeO_2	3	873	100	66	[67]
Co		5.5	693	100	92.6	[68]
	CeO_2				85.0	
	ZrO_2					
3NiCu	ZrO_2	-	873	100	84	[69]
30Ni_2 Zr_3	MCM-48	1	1023	95	85	[70]
$NiGa_3Mg_3$	Zeolite Y	3	973	100	87	[71]
Hydrotalcite						
6NiMg		6	923	100	64.9	[72]
NiMg8	-				64.1	
Co (10)	-	-	923	100	71	[73]
1NiFe	-	6	773	100	80	[74]
$CoMg_2Al$		4	773	100	69.5	[75]
	-					

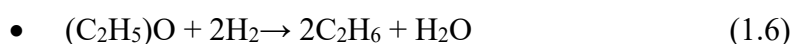|		6	823	100	90	[76]
$Zn_{0.58}Ni_{0.42}[Al_{0.44}$ $Co_{0.56}]_2O$	-					
Spinel						
$NiAl_2O_4$	-	6	823	100	45	[77]
Perovskite						
$La\ Ni_{0.9}\ Cu_{0.3}O_3$	-	6	563	100	37	[78]
$LaNiO_3$	-	13	573	100	70	[79]
Mixed metal oxides						
$Pt_{0.5}Co_{10}$	ZnO	4	598	100	73.2	[80]

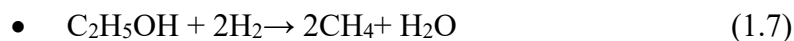## 1.5 Reaction Mechanism of ESR and Carbon Formation

Steam reforming of ethanol may comprise several other simultaneous reactions along with the hydrogen producing reactions. A few of these result in the generation of unwanted products [81-83]. These unwanted products are formed by dehydrogenation (eq1.3), decomposition (eq1.5), dehydration (eq1.9), hydrogenolysis (eq1.7), and aldolic condensation followed by dehydrogenation (eq1.4) of ethanol itself. Acetaldehyde on decarbonylation [84] also produces CH_4 and CO (eq1.8). Ethane can be the major product over a selective catalyst which facilitates ethanol adsorption (leading to diethyl ether formation) followed by hydrogenation (eq1.6) [23, 85, 86]. The reaction network can be written as follows:
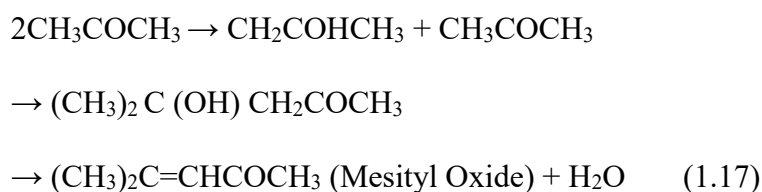
Hydrogen producing:

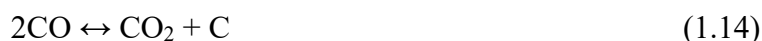- $C_2H_5OH \rightarrow CH_3CHO + H_2$ (1.3)

- $2\ C_2H_5OH + H_2O \rightarrow CH_3COCH_3 + CO_2 + 4H_2$ (1.4)

- $C_2H_5OH \rightarrow CH_4 + CO + H_2$ (1.5)

Hydrogen Consuming:

- $(C_2H_5)O + 2H_2 \rightarrow 2C_2H_6 + H_2O$ (1.6)

- $C_2H_5OH + 2H_2 \rightarrow 2CH_4 + H_2O$ (1.7)

Other reactions:

- $CH_3CHO \rightarrow CH_4 + CO$ (1.8)

- $C_2H_5OH \rightarrow C_2H_4 + H_2O$ (1.9)
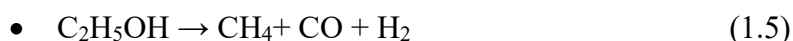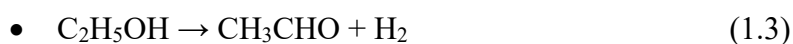
The intermediate reactions during ESR and liable for the carbon deposition on the catalyst surface are as follows [87].

$$C_2H_6 \leftrightarrow 3H_2 + 2C \qquad (1.10)$$

$$C_2H_4 \rightarrow Coke \qquad (1.11)$$

$$C_2H_4 \leftrightarrow 2H_2 + 2C \qquad (1.12)$$

$$CH_4 \leftrightarrow 2H_2 + C \qquad (1.13)$$

$$2CO \leftrightarrow CO_2 + C \qquad (1.14)$$

$$CO + H_2 \leftrightarrow H_2O + C \qquad (1.15)$$

$$CO_2 + 2H_2 \leftrightarrow 2H_2O + C \qquad (1.16)$$

$$2CH_3COCH_3 \rightarrow CH_2COHCH_3 + CH_3COCH_3$$

$$\rightarrow (CH_3)_2 C (OH) CH_2COCH_3$$

$$\rightarrow (CH_3)_2C{=}CHCOCH_3 \text{ (Mesityl Oxide)} + H_2O \qquad (1.17)$$

The reactions (eq1.3-1.9) suggest that saturated, unsaturated hydrocarbons or both can be produced simultaneously during ESR. The dehydrogenation, dehydration, polymerization and decomposition reactions of different byproducts (eq1.10-1.17) are able to generate different forms of carbon. The unsaturated hydrocarbon, C_2H_4 formed after ethanol dehydration, gets polymerized to coke [88] on the surface of catalyst (eq1.11). But the presence of π- bonds in the structure makes them easily disruptive in nature. In a recent review [89], it was pointed out that the decomposition of C_2H_4 occurred at higher temperature but contradicting experimental results showed that even

at the lower temperature (>200°C), the decomposition of C_2H_4 (eq1.12) occurred efficiently [90]. Lower temperature hindered the carbon crystallization during deposition of carbon on the metal surface, especially in presence of carburizing gases because of highly intense C-C bond.

Saturated hydrocarbon such as CH_4 is highly stable and its thermal decomposition (eq1.13) occurs at temperature >1173K [91]. On decomposition, CH_4 is able to generate three kinds of surface carbonaceous species. Firstly, the carbidic species which is highly reactive (hydrogenable at temperature ≈ 323K) and is formed by methane dissociation [49]. It acts as an intermediate in the filamentous carbon growth [81]. During ESR, Co and Cu (over TiO_2 and SiO_2) did not form carbide species but Ni and Fe may form this precursor [92, 93]. The spectroscopic study during hydrogenation of carbidic carbon by He et al. reported that carbon on Ni (100) needs lower decomposition temperature than Ni (111) surface. They suggested that the different form of Ni surfaces (100) and (111) may affect the local structure of CH_x species growth and so thermal stability may be different [94]. However, nickel carbide is not stable and is easy to decompose into metallic as well as graphite form of nickel at high (>873K) temperature [95]. Secondly, amorphous carbon that is less reactive is formed by polymerization of carbidic carbon. It helps to form carbon whisker. Thirdly, the graphite carbon is hydrogenable at temperature around 673K and has different reactivity for oxidation and hydrogenation.

The study over Ni (111) catalyst revealed that carbide formation either in the isolated or string form on the terrace site took place without island formation for C_2H_4. But the growth of carbide formation during Boudouard reaction occurred with island formation. Carbon island consists of graphitic carbon which forms during dissociation of CO on Ni by the diffusion of carbon into the bulk between the metal particles and the

catalyst support [96]. The different ways of growth of carbon are attributed to the dissimilarity in the C_2H_4 and CO dissociation sites [97]. Boudard reaction (eq1.14) is sensitive to the structure of metal in catalyst [98]. The activation energy for CO disproportionation reaction declines by step edge of metal (Ni (111)) but enhances for the associative desorption [99]. Therefore, step edge played a critical role leading the development of carbide species due to dissociation of CO [98].

The hydrogenation reactions of CO (eq1.15) and CO_2 (eq1.16) are favored at high temperature [100]. Thermo-gravimetric analysis of deactivated catalyst during steam reforming of acetic acid over ZrO_2 support suggested that ketene and mesityl oxide is formed due to acetone undergo oligomerization followed by coke formation (eq1.17) [101]. Therefore, the formation of CH_3COCH_3 as an intermediate by-product during ESR may contribute the formation of coke deposition on catalyst surface. Best of the present literature survey, the coke formation due to mesityl oxide and ketene during ESR has not been reported.

1.5. 1 Nature of Carbon Deposit

The carbon deposited on the surface of catalyst during ESR is reported to be of amorphous as well as of filamentous forms [102]. The amorphous carbon contributes more severe deactivation as compared to filamentous carbon [103]. The nanosized carbon filaments such as carbon nanotubes and carbon nanofibers have interlayer spacing equivalent to bulk graphite [104]. Graphitic form of carbon is generated either through the direct deposition of carbon in the vapour phase or through heat treatment of amorphous carbon [104]. Espinal et al. reported the formation of carbon nanotubes on the surface of reacted cobalt hydrotalcite catalyst after performing the ESR [105]. De Bokx

et al. studied production of filamentous carbon from CO and CH_4 over iron and nickel catalyst in the temperature range of 650-1000K and showed that carbon was deposited as a metastable carbon intermediate, leading to filamentous carbon on decomposition [106]. Filamentous carbon has comparatively high mechanical strength and so it has the capability to completely disintegrate the support of catalyst [107]. Typical forms of carbon are shown in Figure1.1. The Figs 1.1(a) and 1.1(b) represent the Ru particles with support and without carbon and encapsulated Ni particle with graphitic layers respectively. The octopus like carbon nano-fibre around Ni crystallite (Figure 1.1(c)) and in carbon nano-fibre at the apex of Ni particle (Figure 1.1(d)) was represented.
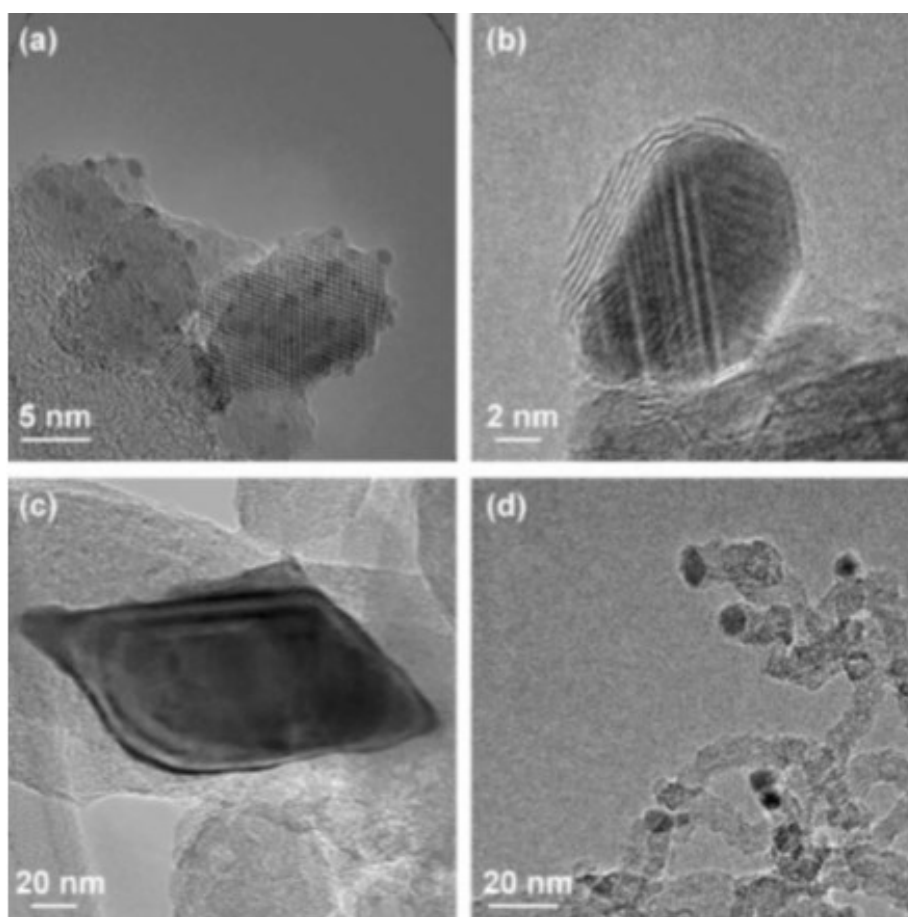

Figure 1.1 Typical forms of carbon formed during ESR.

The spent catalyst characterization with the help of XPS-TPO was unable to reveal the nature of carbon. However, the lower temperature peaks in TPO ascribed the carbon presence in vicinity to the metal, whereas; higher temperature peaks represent carbon existence on the surface of support. The higher and lower temperature oxidation of carbon during Thermogravimetric analysis (TG-TPO) also ascribed for more ordered form (nanotubes and graphitic) and amorphous forms of carbon respectively [108]. Nevertheless, the CO_2 released during TPO cannot be used to differentiate whether it is due to oxidation of carbon deposits or carbonate species [109]. FTIR Raman spectroscopy is best technique to characterize the nature of carbon [110]. Typical spectrum of single walled carbon nanotube suggested lower frequency (<200 cm^{-1}) peak for radial breathing mode. It is absent in graphite carbon. The D band is assigned for a group of peaks around 1340 cm^{-1} as measure of disorder in carbon [111]. The characterization of different form of deposited carbon by FTIR Raman spectra (Figure 1.2) up to 2000 cm^{-1} frequency range was recently reported in few literatures during ESR.
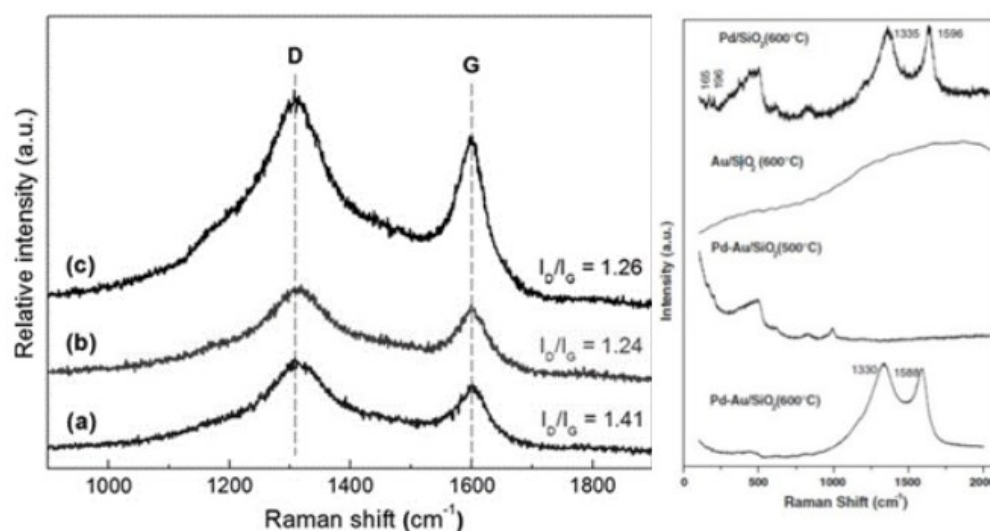

.

Figure 1.2 FTIR raman spectra of typical carbon over different catalyst.

At the low frequency range (165 and 196 cm^{-1}), the peak was reported for carbon nano-tube, whereas, the high frequency range (1,200–1,700 cm^{-1}) was attributed to amorphous and graphitic forms of carbon. Amorphous (disordered) carbon was reported in lower frequency D band (1330-1360 cm^{-1}) as compared to graphitic carbon (ordered) G band (1580-1596 cm^{-1}). Here D band and G-band are attributed to the vibrations of carbon atoms with dangling bonds and the stretching mode of carbon sp^2 bonds, respectively [43]. The single walled carbon nanotube was also suggested by asymmetric G band centred at 1596 cm^{-1}

1.5.2 Carbon synthesis mechanism involved during ESR

The synthesis mechanism responsible for the filamentous carbon formation comprises tip growth mechanism [42]. Frusteri et al., however, suggested that ESR did not involve this phenomena [102]. This statement is irreconcilable since few workers had anticipated tip growth phenomena as a possible growth mechanism [72, 112]. Among these, contradictory studies about carbon growth mechanism during ESR had been reported for catalyst Ni but over a different support.

It emphasizes that support may play a major role in determining the growth mechanism pathway for carbon formation. In this regard, IR spectroscopy studies over growth mechanism during ESR over different catalyst having various supports can be helpful. Moreover, the proposed tip growth mechanism of filamentous carbon formation can be understood by the work of Jeong et al.[90] The root of filament and a large nickel particle are indicated with black and white arrows respectively in Figure 1.3a.The filamentous carbon of different lengths enclosed with Ni (quasi spherical shape) at the tip is shown in Figure 1.3 (b and c).
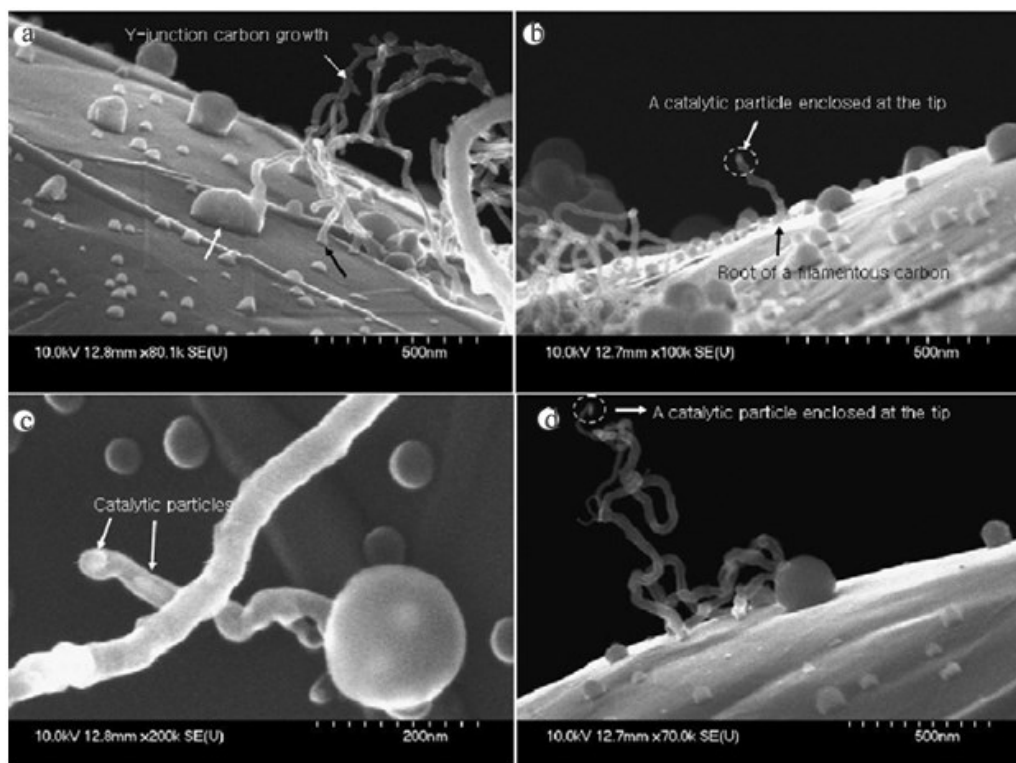
Figure 1.3 Role of nickel nanoparticles in the growth of the filamentous carbon on the surface of the nickel foam. (a) overview of as-grown filamentous carbon, (b) size-dependent growth of a filamentous carbon from a small nickel nanoparticle (<50 nm), (c) size-independent growth of a filamentous carbon from a large nickel nanoparticle (>100 nm), and (d) octopus-like network formation of filamentous carbon.

The surface of quasi-spherical shaped large nickel particles with octopus like carbon network is shown in Figure 1.3d. If the number of fibres grow from a single metal crystal, then it formed the octopus like structure. For the development of highly crystalline carbon on the surface of metal, the carbon atoms need to dissolve as well as diffuse among metal particles. The crystallization must proceed on an appropriate lattice plane help the epitaxial development of carbon crystal [90].
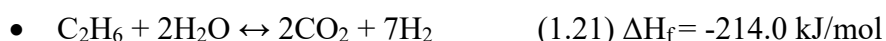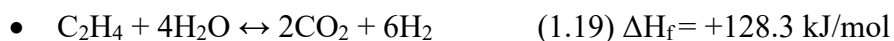
Study of the correlation between size of carbon filament and metal particle size during ESR depicted that larger Ni particle size leads to larger carbon filament. The
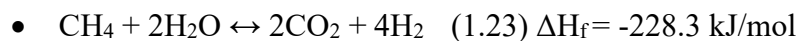
comparison of the nature of carbon formed during ESR and the dry reforming of methane over similar catalyst indicates that the mechanism of the carbon formation in ESR is different from methane reforming [102]. The physical shape of the precipitated carbon depends on the particle size of catalyst as well as precipitation rate. The free energy of less crystalline carbon is comparatively lower than highly crystalline carbon [90].

The deposition of carbon on catalyst surface depends on the site of deposition on the catalyst. The direct deactivation of catalysts occurs principally through the covering of the active phases due to enclosing carbon. During filamentous growth of carbon, deposition occurs on the metal surface and the species made up of carbon move towards the bulk phase of metal which later on saturate and condense. It does not lead to direct deactivation of catalyst but its continuous accumulation blocks the beds [46, 107].

1.5.3 Effect of reaction operating conditions

The operating environment such as water to ethanol ratio (S/C) and temperature during ESR has the crucial role for the carbonaceous deposition. It occurs due to discriminating activities of intermediate hydrocarbon products (CH_4, C_2H_4 and C_2H_6) with temperature and amount of water. These hydrocarbons lead to coke deposition at higher temperature but presence of water facilitates the increase in overall hydrogen yield. It can be clearly observed by the following reactions [113]:

- $C_2H_4 + 2H_2O \leftrightarrow 2CO + 4H_2$ $\qquad$ (1.18) ΔH_f = +210.5 kJ/mol

- $C_2H_4 + 4H_2O \leftrightarrow 2CO_2 + 6H_2$ $\qquad$ (1.19) ΔH_f = +128.3 kJ/mol

- $C_2H_6 + 2H_2O \leftrightarrow 2CO + 5H_2$ $\qquad$ (1.20) ΔH_f = +352.0 kJ/mol

- $C_2H_6 + 2H_2O \leftrightarrow 2CO_2 + 7H_2$ $\qquad$ (1.21) ΔH_f = -214.0 kJ/mol

- $CH_4 + H_2O \leftrightarrow CO + 3H_2$ $\qquad$ (1.22) ΔH_f = +206.3 kJ/mol

- $CH_4 + 2H_2O \leftrightarrow 2CO_2 + 4H_2$ (1.23) ΔH_f= -228.3 kJ/mol

Therefore, molar ratio of ethanol and water in the feed during ESR has significant role on the suppression of carbon deposition. It can influence the yield, selectivity and deactivation of catalyst. At high temperature water gas shift reaction leads to increase in hydrogen productivity and decreasing carbon deposition although it requires high energy consumption [100]. The concentration of water, higher than stoichiometric quantity was reported to have an inhibitory effect on coke formation [114, 115]. This statement is also supported by the experiment of different molar ratio concentration over Rh catalyst for 100h time on stream. Molar ratio of water and ethanol lower than stoichiometric ratio showed deactivation within 4h of operation. The antagonistic effect of higher ethanol to steam ratio for ESR was experimentally approved over Ni catalyst on various support (La_2O_3, γ -Al_2O_3, La_2O_3/γ -Al_2O_3) [96]. Thermodynamic analysis depicted that rate of coking was very low for molar ratio of water and ethanol higher than 10:1 [116]. It is also noteworthy that the thermodynamic equilibrium calculations of ethanol dehydration at 873K suggested that the product should be altered towards ethane and water despite of the water content [117]. It implies the importance of acidic, basic or neutral nature of support regarding the effect of S/C ratio during ESR. However, the effect of S/C ratio was studied till now mainly over acidic support. Therefore, the study of S/C optimization over different nature of support may lighten the information about its exact contribution in the carbonaceous deposition.

Temperature plays an important role in carbon deposition but the available information is that the carbon deposition is governed by different kinds of reactions at different temperatures and hence is not so consistent. At lower temperature, Boudard reaction and hydrogenation of CO are the dominant reactions facilitating the carbon

formation. Whereas, at high temperature, boudard reaction reversed but carbon deposition facilitates through decomposition of hydrocarbons (eqs 1.10, 1.12 and 1.13) [29, 118, 119]. Therefore, the intermediate reactions responsible for deposition of carbon are different at different temperatures. It had been reported that usually for Ni catalysts, high temperature facilitated the carbon deposition [120-122], whereas, in case of Rh catalysts, the rate of carbon formation is increased with lowering of temperature [115]. These two contradictory statements concerning temperature indicate that owing to the diverse reaction pathways, depending on catalysts during ESR, the intermediate reactions might be different and hence, it showed a typical performance with respect to temperature. Recently, the uniformity of heating temperature for catalytic bed was also reported as contributor for coke formation during ESR. Microwave heating was confirmed as a better option comparative to conventionally heated reactor [123]. Besides, these parameters effect of inert atmosphere has also seen a role in coke deposition over catalyst surface. It acts as remover of less dense coke formed during ESR over catalyst surfaces [124]. However, its role is less vital as compared to temperature and S/C ratio.

1.5.4 Effect of catalyst preparation conditions (precursor and methods)

The effect of nature of catalyst precursor used for the preparation of catalyst contributes to the carbon deposition. The work reported by Galetti et al.(2011) over nature of catalyst precursor revealed that the nitrate salt precursor used for catalyst preparation via impregnation method exhibited most carbon resistance characteristics. The authors supposed that in the inorganic precursor derived catalyst, deactivation occurs due to active carbon (C-C), whereas, the nickel acetate precursor used for catalyst preparation led to the formation of -CO-C- inactive species during ESR. Therefore, catalyst deactivation becomes more severe for the catalyst derived from organic precursors. The

catalyst calcined under reductive atmosphere was also found to be more stable compared to the catalyst calcined under oxidative atmosphere [125].

Preparation methods govern the dispersion of active phase or stronger metal support instauration interaction. It confines the coke filaments formation during low temperature ESR [108]. Effect of support (SiO_2) preparation method on carbon deposition was carried out by Rossetti et al [51]. The liquid phase synthesis of support only showed silanols responsible for deposition of carbon. Moreover, the Lewis acid sites were also detected in the support prepared by flame pyrolysis method and so were responsible for the dehydration of ethanol leading to coke deposition. The catalyst prepared by sol-gel method showed the effect of citric acid concentration used during catalyst preparation on coke formation. It was increased with the increasing citric acid content in the sol–gel preparation process. The optimization of citric acid during catalyst preparation is also noteworthy as lower concentration of citric acid leads to deactivation due to sintering [112]. Effect of citric acid concentration on coke deposition is associated with the surface area of catalyst as indicated by the work of Takahashi et al [120]. Citric acid makes hydrogen bond with silanol during preparation of silica supported catalyst via sol-gel method. Therefore, high citric acid concentration leads to collapse of space occupied on calcination in the catalyst precursor and ultimately resulted into broad pore size distribution. However, diversity of carbon formation was not correlated with citric acid concentration.

Wurzler et al. [126] were recently reported that during precipitation method of catalyst precipitating, aging has significant role to increase the basicity. The better distribution of NiO with MgO, highest reduction degree and basicity lead to decline in coke formation [126]. The homogenous dispersion and smaller size of metal clusters

through redistribution of metals or lowering of metal valency can be induced by non-thermal plasma treatment. Redistribution of metals check the blockage of pores of catalyst and so coke deposition got reduced. Wu et al [127] used the dielectric barrier charge after calcinations of Ni/γ-Al$_2$O$_3$ catalyst and found relatively more catalytic activity with 97% carbon balance as compared to untreated one at 810K [127].

1.6 Catalyst Modification Strategy:

There are several approaches to minimize carbon deposition during ESR, such as increasing water to ethanol ratio; auto-thermal steam reforming, co-feeding either H$_2$ or CO$_2$ and catalyst modification. Increase in water to ethanol ratio requires high temperature to facilitate the reaction. Auto-thermal steam reforming is an exothermic reaction but overall yield of hydrogen gets reduced compared to ESR. Co-feeding of CO$_2$ at lower temperature reduces the carbon deposition up to certain extent but competition with ethanol adsorption at common site is major disadvantage of this approach. The hydrogenation of deposited carbon reduces the deactivation but it facilitates the hydrocarbon yield in spite of H$_2$. Therefore, catalysts modification strategy has shown better possibility in minimizing the carbon deactivation during ESR in terms of yield as well as cost. Catalyst formulation must require knowledge of activity of metals, support and synergistic interactions between metals along with their support during ESR for the carbon generation and deposition.

1.6.1 Active metals

The noble metals are more resistant to carbon deactivation compared to non-noble metals. Among noble metals, Rh is highly active for both C-C and C-H bond scission [23]. It induces hydrogenation reaction and leads to very low carbon deposition [128]. It

also has the ability to evade carbonate formation that's why the oxygen vacancies are easily accessible for oxidizing carbon [129]. Carbon formation was reported insignificantly for Rh at stoichiometric molar ratio of water and ethanol [34]. Nevertheless, Pt catalyst over different oxide supports (CeO_2, Al_2O_3, ZrO_2) during ESR showed significant amount of carbon deposition [20]. Comparative study of ESR on Au and Pd catalyst over SiO_2 support revealed Au to be more stable compared to Pd [130]. The catalyst Ir over CeO_2 at low temperature (623K) and PrO_x doped CeO_2 up to 923K did not show deactivation during ESR [66, 131, 132]. Ru provokes the ethane formation via ethanol dehydration and ultimately results in coke formation. Though, study of nano sized Ru, Pd and Ag over mixed oxide (CeO_2/YSZ) support revealed the order of stability towards carbon as Ru >Pd>>Ag [18]. Overall, the carbon depositions as compared to non-noble metals are considerably less.

Pure Ni has the ability to cleave the bond of ethanol in the order of O–H, $-CH_2-$, C–C, and $-CH_3$ [133, 134]. Coke formation is strongly depressed due to the benefits induced by the use of basic carrier which positively modified the electronic properties of supported Ni [135]. Skeletal Ni based catalyst has large exposed surface area and high dispersion of Ni, so it is also useful in reducing carbon deposition [136]. If catalyst is deficient of the support and metal interaction then it leads to significant amount of filamentous carbon whisker [137]. Study of temperature program reduction showed that reduction of NiO is easy if the interaction between the support and metal is weak. But it is not only facile to be sintered but also resulted in formation in larger particles, vulnerable for carbon formation. Promotion of the C-C bond splitting imparted by Ni is not efficient at low temperature. Therefore, acetaldehyde decarbonylation and aldol

condensation reactions compete with each other and basic properties of support lead to further generation of acetone [138].

Cobalt catalysts are predominantly active at low temperature and enhance the water gas shift reactions [92]. Existences of Co^{2+} species facilitate ESR, whereas the metallic cobalt leads to the deposition of carbon over catalyst surface [105]. Because the metallic form favours decarbonylation of adsorbed ethoxy species, Co^{2+} is efficient for dehydrogenation reactions [139]. It is highly active for C-C bond cleavage [140-142]. Even at low temperature (673K), performance equivalent to noble metal catalyst in terms of C-C bond scission was reported for supported cobalt [143, 144]. However, few authors had found Ni over γ-Al_2O_3 and ZrO_2 support to be more active catalyst compared to Co [90].

The Cu based catalysts had poor catalytic activity for the steam reforming of ethanol. Cu has good catalytic property for dehydrogenation but is ineffective in the cleavage of C-C bonds. It formed high concentrations of intermediates such as acetaldehyde and ethylene [145-147]. However, at lower temperature (623K) Cu showed more stability towards coke deposition as compared to Ni [90].

1.6.2 Bimetallic interaction

Monometallic catalysts had solitary catalytic nature while synergistic interaction between the two metal components of a bimetallic catalyst may have beneficial effect on carbon deactivation during ESR [148]. The noble metal is comparatively more active but due to cost issue, addition of smaller amount of these metals with non-noble metals are used to improve the stability. Therefore significant research work was carried out to find out the interaction between noble and non-noble metal catalysts. If Pt is segregated

toward Ni particle surface through bimetallic interaction than rate of hydrogenation of the adsorbed carbon species at the surface increases relative to its (carbon) diffusion into bulk nickel [149]. The Co with Rh metal catalysts mutually over ZrO_2 and CeO_2 support were reported to be less prone to catalyst deactivation compared to monometallic cobalt catalyst [150, 151]. Moreover, Rh and Ni bimetal over CeZr oxide support showed lower carbon filament formation due to increase in Ni reducibility and its dispersion [152]. The Cu and Ni is particularly efficient in catalysing water gas shift reaction [153]. Fierro et. al.[87] suggested that on addition of Cu, the large ensembles of Ni metal atoms extinguished, melting temperature turned out to be average; existing state of Ni altered and the affinity with carbon gets changed. It formed a NiCu solution and resulted into lower deposition of carbon by CH_4 decomposition [145, 154]. Stability of catalyst with reference to activation of C-C and C-H bonds gets lowered by partial substitution of Ni with Cu. But, it favoured the formation of low-volatility polymers owing to condensation reactions of acetaldehyde and other intermediates [138]. The synergistic effect of Ni and W was reported over SBA-15 and ceria. Inside CeO_2, the structure due to the difference in preferable coordination number of Ni, W (6) and Ce (8), electronic and structural perturbation increased substantially. W and Ni promote the Ce^{3+} site formation and it increases the –OH species on the surface of catalyst due to partial dissociation of water. Ultimately, it leads to oxidation of CH_x species and lowers down the coke formation [155]. The suggested model states that CH_4 and CO formation occurred over Ni sites and further CH_4 reforming and CO-Water gas shift reaction occurred over NiO and Ni-W alloy sites respectively [156].

Easily combustible coke is easy to remove and its formation depends on the metal catalyst on which ethanol gets adsorbed or desorbed. Hence, different kind of coke in

terms of reactivity towards combustion on metal was reported on Ni and Co monometallic as well as spinel catalysts. This reactivity was reported in order the 10%Co > 3.3%Ni 6.7%Co > 6.7%Ni 3.3%Co > 10%Ni and therefore, higher activity of Co catalyst as compared to Ni over γ-Al$_2$O$_3$ support. The amorphous and filamentous nature of carbon was also reported over Co and Ni respectively on study of Ni-Co alloy nano particles supported over La$_2$O$_3$ [103]. Since Ni has strong capability to break C-C bond as compared to Co, carbon deposited on Ni was more crystalline and difficult to burn out compared to that on Co [90]. Ni is more efficient to break C-C bond compared to Co, whereas Co leads to formation of less stable coke, therefore optimum concentration of bimetallic catalyst formulation may result into highly efficient and stable catalyst. Moretti et al. [157] had found the synergistic effect of Co and Ni over Ce/Zr (9:1) support as an increment of reducibility of both metal phases [157]. Recently, Zhao et al. [158] studied the bimetallic Ni- Co alloy perovskite catalyst supported by ZrO$_2$ and it had been found that bimetallic perovskite had better anti-sintering and anti-coking ability as compared to their monometallic perovskite form [158]. Zhang et al. [41] had conducted the low temperature ESR over skeletal Ni based catalyst and reported that bimetallic catalyst Cu–Ni, Co–Ni, and Pt–Ni did not show any C$_2$ or C$_3$ species on their surface due to the promoting effect of these bimetallic catalysts [41]. Low temperature steam reforming and less amount of amorphous carbon has been reported compared to that for supported nickel nano-particle catalysts. The carbon deposited is considered to be formed by decomposition of methane [136]. The decomposition of methane, most apparently occurs if the high density of nickel d-state which is near to Fermi level, interacts with the vacant anti bonding orbitals of C-H bond. The element such as Au which is able to lower the d-band state reduced the interaction of anti-bonding orbital and d- state. So, the alloy

formation with such element is beneficial reducing coking on Ni atom [159]. A model was proposed by using Ni and Mo bimetals over SBA-15 support. It states that conversion of ethanol into acetaldehyde and acetaldehyde into CH_4 and CO over Ni active sites and CH_4 reforming over Mo sites leads to deduction in carbonaceous deposition [160]. Kim et al. [160] proposed the model of two bimetallic catalysts over common support SBA-15. They had stated that Mo has higher efficiency to adsorb CH_4. Therefore, the parallel side reaction as a methane steam reforming will occur at the surface of Mo for NiMo bimetallic catalyst. Nevertheless, methane steam reforming will be prominently occurred over Ni in case of NiW bimetallic catalyst. Aforementioned, both the proposed model mechanisms of ESR over bimetallic Ni based catalyst over SBA-15 are collectively illustrated in Figure 1.4.
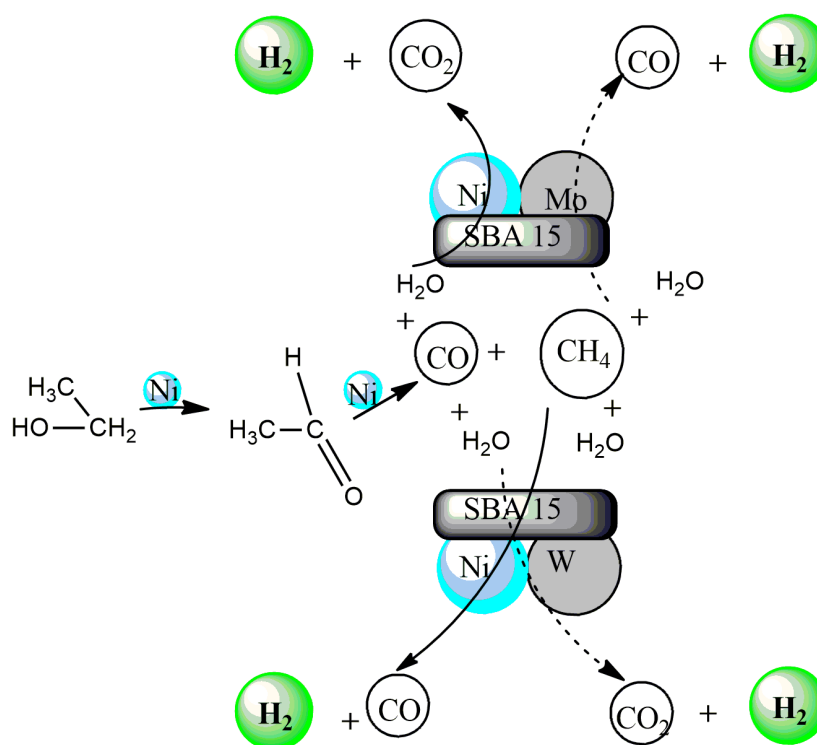

Figure 1.4 The proposed model mechanisms of ESR over bimettalic Ni based catalyst over SBA-15 support.

1.6.3 Support

Catalyst support plays significant role during ESR[30] and takes part in the generation of carbon over catalyst surface. The strong interaction between metal and support leads to lower generation of carbon [161]. A number of workers studied ESR on the noble and non-noble metal over different kinds of oxide support such as Al_2O_3, CeO_2, ZnO, MgO, ZrO_2 and SiO_2 with variation of metal loading. Lot of literature is available on the study with ZnO and MgO but is less specific in terms of their carbon stability [88, 102, 135, 139, 141, 146, 162-170]. Temperature program desorption study showed that coking was affected by supported metal. The low temperature study of Pt catalyst over different support had shown carbon deactivation in the order $CeO_2 >> Al_2O_3 > ZrO_2$ indicating that the nature of the metal oxide support has significant contribution in favor of carbon deposition.

1.6.3.1 Alumina

Alumina is a highly mechanical as well as thermally stable metal oxide. It acts as an acidic support in catalytic reactions due to the acidic centers present on its surface. Therefore, it promotes dehydration of ethanol and leads to ethylene formation [55]. It is responsible for coke deposition in highly active carbon form and is easy to oxidize. To reduce the coke deposition by increasing the surface area, the spherical catalyst Ni/Al_2O_3 was reported with the help of chitosan and Al solution [171]. However, during ESR on prepared catalyst CO was missing but other coke forming intermediate product, C_2H_4 was detected. If ZnO is mixed with Al_2O_3, then it not only removes the acidic centers but also creates some Lewis acidity and thus promotes ethylene selectivity [102]. If Zn reacts with

Al_2O_3, it forms zinc aluminate. Ultimately, it distorts the structure as well as surface chemistry of the catalyst. Catalytic properties of the catalyst's active phase can also be altered by the reduction of zinc oxide into metallic zinc. If the reduction temperature for nickel and zinc oxide is not sufficient to reduce all Ni (II) and Zn(II) in $ZnAl_2O_4$, then it promotes water gas shift reaction and so production of CO is lowered [172].

The temperature programed oxidation of ZrO_2 and Ca-γ-Al_2O_3 supported catalyst reported by Chen et al. [90] was indicated that ZrO_2 is more prone to the formation of C_2H_4 at any temperature compared to Ca-γ-Al_2O_3 [90]. The major drawback of Ca addition in Al_2O_3 supported Ni catalyst is that it decreases the strength of bond between Ni and Al_2O_3. On the other hand, the benefit of Ca is that its addition favours declining of acid sites owing to decrease in the surface area of Al_2O_3. It leads to the alteration in the reactivity and stability. Calcium has availability of electrons to enrich the Ni 3d-band electrons. Hence, the loading of Ca promotes electron enrichment on the Ni metal. The decomposition of methane got enhanced with Ca doped catalyst. Choong et al.[173] had reported the trend of coking rate with 10% loaded Ni catalyst on Al_2O_3 with varying Ca loading (wt. %). The order sequence was Ni/7Ca- Al_2O_3> Ni/3Ca- Al_2O_3> Ni/Ca-Al_2O_3. The crystalline nature of carbon was found and so it was easily gasified. The optimum loading was reported as 3% under consideration that coke deposited by CH_4 decomposition is reduced at the steady state of coke gasification deposits.

Silver addition on Ni/Al_2O_3 was reported to have an inverse effect on the inhibition of carbon deposition. The reason behind this pessimistic action is the decrease in Ni sites resulting in less coordination between metal and ethanol. According to Liberatori et al. activation of ethanol molecules on the surface of metal is relatively easier

than that of methane [174]. Therefore, the coordination of Ni sites is not responsible for the activation of ethanol.

1.6.3.2 Silica

The novel work on cobalt-talc nano layers dispersed in silica aerogel for efficient hydrogen production via ESR was reported but not with reference to carbon deposition [175]. The comparative study of Co supported on SiO_2 and Al_2O_3 revealed that the type of carbon formation may be controlled by the particle size [176]. This study was also supported by the work of Lee et al.[177]. It had been reported that in case of Ni catalyst, smaller size particles facilitate the synthesis of filamentous form of carbon with a slower rate because of the low driving force for carbon diffusion through the small crystals. The maximum amount of filamentous carbon was reported for Co catalyst supported on Al_2O_3 compared to SiO_2 support, owing to acid sites of alumina. Chen et al. [90] had also found that the yield of carbon nano-fibre (CNF) is extremely sensitive to Ni (NiO) crystal size and the yield of the CNF increased with Ni crystal size at a certain range [90]. Optimum ratio of Cu / Ni ≥ 1 on SiO_2 support was suggested by Chen et al. for the low tendency of carbon and scission of C-C bond energetically [90]. Furthermore, addition of Ca and Mg generate defective disordered carbon leading to lower stability and easier thermodynamic removal during steam reforming of ethanol.

1.6.3.3 Ceria

The catalyst support having high oxygen storage capability leads to oxidation of deposited carbon on the surface of catalyst. CeO_2 has efficient oxygen vacancies but its catalytic property is unstable at temperatures higher than 673K. During ESR high oxygen defects with mobility is prerequisite for better activity and stability of catalysts [178]. It

has reversible change oxidation state (Ce^{4+}/Ce^{3+}) ability and so it is able to exchange oxygen much efficiently [179]. The effect of doping of Ca, Pr, Fe and Zr in CeO_2 was studied for ESR [180-183]. Small addition of Fe, Pr, Zr and over 5% Ca addition in CeO_2 not only promotes the reduction ability but also enhances the surface area and oxygen vacancies. Addition of Ca also minimizes the particle size of ceria in Co/ CeO_2 catalyst and Zirconium addition elevate the thermal stability to CeO_2. Recently, Wang et al. had reported that small addition of Ce with Ni/SBA-15 facilitate the dispersion of active metal and strengthen the metal support interaction. It enhance, the anti-coking ability significantly [184].

Morphology and size of CeO_2 has also a great role in ESR, especially for anti-carbon deposition. Because the potential of oxygen vacancies concerned to morphology and the different plane (100) as well as (110) of ceria [185]. Furthermore, study of ESR on nanorods and nanoparticles of CeO_2 with Co suggest nanorods of CeO_2 as a better option with respect to carbon deposition as well as oxygen vacancies. Soyakal et al.[186] used Co supported on nanoparticles and nanocubes of CeO_2. The nanocubes of CeO_2 support showed higher oxygen mobility and higher density of surface basic sites. The Ni catalyst over (10%) CeO_2 modified $ZnAl_2O_4$ spinel had capability to induce 50% reduction in carbon formation on the catalyst [43]. When ceria is doped with nickel, it creates oxygen vacancies and Ce (III) sites which had comparatively higher atomic radii than Ce (IV) sites.

1.6.3.4 Titania

Titanium oxide is typically used in photocatalytic hydrogen generation from ethanol or water [12, 13, 187]. However, carbonaceous deposition is not an issue in

photocatalytic conversion of ethanol to hydrogen, but C-C bond scission at ambient condition is still a challenge to increase the hydrogen yield [188]. Titanium oxide exists in three phases viz. rutile, anatase and brookite [189]. In photocatalytic activity, rutile phase is comparatively less active than anatase. Infrared spectroscopic study of ethanol on different temperature suggests that over rutile phase at 523K, ethanol decomposition was favoured. But the rise in temperature from 573 to 673K leads ethane production trace to major product. Recently, the Ni catalyst over TiO_2 dominant with nano crystalline anatase was reported for ESR. The coking was significantly occurred due to the lewis acidity of support [190].

Overall, the acidic property of support promotes the carbon deposition owing to dehydration of ethanol. So, the selectivity of ethylene increases with lewis acidity of support. Decomposition or gasification of the polymerized coke needs optimum metal and support interaction otherwise it hindered the ESR. Therefore, decreasing acid sites on support means reduction of coke formation but not at the cost of metal support interaction as it resulted into lower availability of active metal in the reaction. Furthermore, the size of particle also affects the nature of carbon because the smaller size of particle have slower rate of carbon deposition and so filamentous carbon facilitated during ESR.

1.6.4 Doping with other metals

The effect of doping in catalyst may be inhibitory as well as facilitative in terms of carbon deposition [167, 173, 191]. The addition of basic solid into acidic support decreases the rate of coking [191, 192]. This statement was contradicted by Moura et al.[193, 194]. However, the effect of doping was compared with the catalysts used for the

steam reforming of other source of hydrocarbon (CH_4) in place of ethanol. The different source of hydrocarbon has different role in the growth of carbon [50]. Therefore, study about doping of metal effect over catalyst during ESR is very essential.

1.6.4.1 Zirconium addition

ZrO_2 itself has been used as a support in catalytic reactions but low surface area and weak mechanical stability make it inappropriate for ESR. Whereas, the stability of Al_2O_3 supported catalyst gets intensified on addition of ZrO_2 because of its property to increase the adsorption as well as dissociation of water on the surface of nickel catalysts. The capability of support for the H_2O adsorption decides the reaction pathway involved which leads to product selectivity followed by carbon deposition. Water-gas shift reaction on the catalyst surface increases with increase in acidity due to adsorption of higher number of CO species [195]. Ultimately, a surplus amount of ZrO_2 lowers down water-gas shift reaction in the steam reforming of ethanol.

Zirconium also decreases the surface area but enhances the reducibility and eventually decreasing the acid sites of catalyst. Effect of Zr/Al molar ratio in $Ni-Al_2O_3-ZrO_2$ xerogel catalyst revealed that surface area and interaction between support ($Al_2O_3-ZrO_2$) and nickel oxide both were inversely related to molar ratio. Reduction of surface area occurred because Zr^{4+} ion has comparatively larger radius than Al^{3+} ion, therefore incorporation of aluminum ions into ZrO_2 leads to lattice contraction [196]. The lower interaction between metal and support occurred owing to formation of the composite structure of $NiO-Al_2O_3-ZrO_2$ [197]. It has been also reported that in the aforementioned catalyst, the coking culprit reactions i.e ethanol dehydration and ethylene formation reactions also get reduced [173].

1.6.4.2 Lanthanum addition

Lanthanum has been shown to reduce the carbon deposition over Ni catalysts [96, 174, 198]. It oxidized the adsorbed carbon to CO by means of lanthanum oxycarbonate and ultimately hampered the carbon island [147, 199, 200].

$$La_2O_2CO_3 + 2C \rightarrow La_2O_3 + 2CO \qquad (1.24)$$
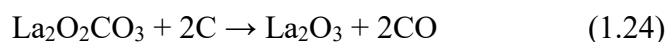
Lanthanum forms perovskite structure with active non noble metals such as Ni, Co, Fe etc. The strong interaction of highly dispersed Ni-Fe alloy with disordered perovskite matrix compels perovskite derived catalyst as a better coking stability rather than perovskite supported one [201]. Lanthanum is also able to obstruct the graphitic carbon formation on the catalyst surface and impregnation of La_2O_3 over Al_2O_3 reduces the rate of coking [96]. The addition of lanthanum in acidic supports reduced the activity associated with their acidic sites. La_2O_3 contributes to the activity, supports the aldol condensation or dehydrogenation reactions during ESR. Moreover, La_2O_3 has the tendency to use the water and is liable to deform the structure [202]. Doping of lanthanum into Al_2O_3 shows incorporation of two dimensional well scattered entities on characterization of supports. Study of interaction between Ni and La atoms suggested that the close contact between these two atoms could enhance the obstruction of Ni sites, responsible for ethylene dehydrogenation. Sanchezsanchez et al.[203] reported the alteration at the surface of Al_2O_3 with lanthanum resulting in increase in the dispersion and stability of nickel metallic phases on addition of La. The contradictory result was also been reported by Melchor-Hernandez et al.[199], that progressive incorporation of La apparently promotes the appearance of NiO species having weak interaction with the support.

The study on Ag and La promoted Ni/Al$_2$O$_3$ catalyst depicted that Ag strongly deformed the Ni surface but was unable to suppress the coke formation, whereas, La was able to decrease the coking. Lanthanum promoted Ni/Al$_2$O$_3$ catalyst has been shown to be highly susceptible to oxidation by water compared to unsupported catalyst[174]. The Co over MgAl$_2$O$_4$ doped with La, Ce and Pr shows similar quantity of carbon deposition. However TG analysis of Ce and Pr doped catalyst confirm lesser burning temperature than La doped catalyst. Authors suggested that it may be due to difference in the fiber structure that is parallel (a center hole and the metallic particle on the tip) or fishbone type. The region of support containing Co and La showed high amount of coke deposition [204] on the spent catalyst.

1.6.4.3 Alkali and alkaline earth metals

As it is well known that acidic supports promote formation of coke precursors, hence the introduction of basic carrier such as alkali (Li, Na, K and Cs) and alkaline metals (Ca, Mg and Sr) to neutralize acid sites has been suggested as an effective approach [205]. Intermediate hydrocarbons (such as methane and ethylene formed during ESR) decomposition and Boudouard reaction also get supressed by alkali metals, because they are able to provoke an electronic enrichment on the active phase of catalyst surface.

Integration of CaO and MgO has been shown to decrease the amount of coke deposition as well as alter the nature of coke [206, 207]. The initial rate of coke synthesis got enhanced for the catalyst doped with promoters (Mg and Ca), whereas, over the long deactivation period, quantitatively the coke formed on the surface of catalyst with promoter was reported to be lower compared to the catalyst without promoter [208]. The Ni/Al$_2$O$_3$ catalyst synthesized with the lamellar double hydroxides (LDHs) as precursors

contained extremely dispersed metal particles in an aluminium structure. Furthermore, addition of Mg with Mg/Ni ratio more than 0.1 to Ni(II)Al(III), precursor resulted in very high activity with low amount of coke deposition (reduced up to 25 wt.%), because of hindrance in ethanol dehydration [209]. Among alkaline earth metals, Mg and Ca both promote the catalytic properties of Ni/α-Al$_2$O$_3$ but Mg only was reported to alter the Ni particles. Mg inhibits the synthesis of less reactive coke because it blocks the pathway essential for the nucleation of graphene. Moreover, the promotion characteristics of Ca were suggested due to its ability to increase gasification of adsorbed carbon [206, 210]. The contrasting result was reported about the role of Ca and Mg for carbon deactivation on Cu-Ni bimetallic catalyst supported over SiO$_2$. It was suggested that Ca modified catalyst generates lower carbon deposition as compared to Mg modified catalyst due to increase in basicity as well as a reduction in active phase particle size [40]. However, both of these contradictory results suggested that either acidity of support or synergistic effect of two metals might play a major role for the efficiency of these doped alkaline earth metals to reduce carbon deactivation during ESR. Moreover, the study of Mg and Ca addition with SBA-15 were studied with Ni and Co active metals. It was reported that Mg and Ca both had not common coke reduction with both of the active metals. The prominent reduction in coke formation was found for Mg with Co and Ca with Ni [211]. It indicates some active and doped metal interaction role in the dispersion or metal support interaction which effects the coking ability of catalysts.

Among alkali metals, effect of Li, Na and K doping on Ni/MgO catalyst had been studied. It was revealed that morphology and dispersion is not significantly affected by K, whereas, Li and Na inversely affected the dispersion of the Ni/MgO catalyst, but support the reduction of NiO. The rate of formation of carbon species for bare and alkali-

doped Ni/MgO systems was reported to be relatively slower than Ni catalyst supported on acidic carrier [102]. Besides these, optimum doping[212] of K (0.5%) over Ni/MgAl$_2$O$_4$ leads to blocking of the step-site of metal catalyst as well as elevate the steam adsorption on the catalyst surface and so ultimately reduce the carbon formation [213]. Potassium is also able to hamper the CH$_4$ dehydrogenation and retard the deposition of coke over Ni catalyst supported on alumina [214]. It has been revealed from CO chemisorption followed by FTIR characterization that addition of Na might block the active sites of Co. Initially, rate of dehydrogenation decreases for (0.98 %) Na doped Co/ZnO catalyst, but the deactivation of catalyst got reduced [170]. Oxide supports are capable of water adsorption which leads to the coke gasification especially at higher temperature and so activate the catalysts [107]. The addition of alkali and alkaline earth metals act as a promoter for generation of large number of adsorption sites for water [173].

1.6.4.4 Yttria addition

Different molar ratios of Y: Al were used to prepare Y$_2$O$_3$-Al$_2$O$_3$ support for Ni metal and used for ethanol steam reforming. The catalyst with 1:1 molar ratio of Y: Al showed comparatively less carbon deposition on the reactant catalyst. It occurs due to suitable interface between the composite support and NiO resulting in easy reduction of NiO. So, the active oxygen species and active sites form abundantly over the composite supported catalysts. The synergistic effect between support and active constituent could be persuaded by different mole ratio of Y and Al in the support [215].

1.6.5 Metal nanoparticles on supports

The catalysts of smaller size used during ESR not only increase the conversion [68] but also decrease the carbonaceous deposition. But the temperature is limiting parameters as the nanoparticles are more prone to get sintered at high temperature and lead to coke deposition [190]. Hence, the roles of support with nano active metal particles become very important matter of concern. The carbon filament formation is typically interrelated with dispersion of metal particles on support. The metal nanoparticles with support reduce carbon filament formation during ESR. The similar dispersion of Ni particle reported as analogous coking behaviour and an opposite trend of Ni crystal size with C balance [216, 217]. The nickel crystal with larger size generates higher amount of nanotube formation during ESR [108]. Recently, a few works have been reported with active nano metal catalysts. The nano size Rh particles over SiO_2 with 15% La_2O_3 doping have shown very low deposition of carbon [218]. The nano-NiO/SiO_2 with optimum (10.28 wt.%) loading over Al_2O_3 support remains stable for the long period [219]. The work over noble metals (Ru, Pd and Ag) nano-composite was also reported over CeO_2/YSZ support [18]. The Ru and Pd based catalyst shows very low coke deposition and the location and morphology of the coke deposition also depends on the metal. The nano composite formation did not affect the pore structure of support because it substitutes the part of support matrix. Therefore, it ultimately increase the surface area and metal support interaction [220]. The cobalt and nickel nanoparticle over alumina support also have comparatively lower carbon deposition with respect to larger one [221, 222].

The Table 1.2 presents summary of the available literature comparing the amount of carbon deposited during ESR. These were reported by earlier workers using different catalysts and supports and effecting operative parameters. It has been represented to find out the correlation among the different type of metals (noble and non-noble metal), bimetallic interaction, particular support and mixed oxide support for carbonaceous deposition during ESR. There are only a few works reported on the catalyst deactivation and their characterization, especially in terms of the amount of carbon. Most of the authors had described the stability on comparing the experimentally performed data of their catalyst in terms of relativity in stability of catalyst. The data was also found with different time on stream (TOS) over different temperature. The amount of water in feed mixture was also taken randomly or stoichiometric requisite basis by several authors. Therefore, a number of variations in operating parameters which has a major role in catalyst deactivation cannot lead to an absolute interrelated conclusion. The quantity of carbonaceous deposition was reported as g_c g_{cat}^{-1} with different time on stream. But few authors used the term deactivation rate (g_c g_{cat}^{-1} h^{-1}). The rate of carbon deposition may vary with TOS [218]. Since, if the carbonaceous deposition is able to block the active sites of metal catalyst then it will lead to higher rate of coke deposition with TOS compared to the unblocked active site containing catalyst surface. The work reported by authors especially in the recent past is significant and noteworthy regarding various aspects of catalysts deactivation [223-229]. Overall, Rh has been reported negligible carbon deposition even with Al_2O_3 based catalyst and among non- noble metals Co and Ni or its bimetallic effect with CeO_2, mixed oxide or Special structural catalyst (spinel) has shown significant capabilities to reduce coke deposition during ESR.

Table 1.2 Carbon deposition during ESR over different types of catalyst.

Catalyst Active metal	Support	H_2O/EtOH	Temperature(K)	Carbon ($g_C g_{cat}^{-1} h^{-1}$)	References
Rh	Al_2O_3	8.4	923	0.0027	[128]
Rh	Al_2O_3	6	859	10.57^	[230]
Ni	Al_2O_3	13	773	0.103	[215]
Ni	SiO_2	3.5	873	0.37 (TOS:6h)	[64]
Ni	SiO_2-0.5[!]			0.007* (TOS:2h)	[112]
	SiO_2-1.0[!]			0.009*(TOS:2h)	
	SiO_2-1.5[!]			0.032*(TOS:2h)	
	SiO_2-2.0[!]			0.053*(TOS:2h)	
	SiO_2-3.0[!]			0.075*(TOS:2h)	
Ni	CeO_2	5.8	865	0.018	[117]
Ni	ZrO_2	3	773	0.0101	[216]
	ZrO_2 with Ca (9)			0.0075	
Ni	ZrO_2	3	573	0.018	[231]
Co	SiO_2	3	773	0.008	
Co	Al_2O_3	3	773	0.29	[232]
Co	α- Al_2O_3	5	823	0.418* (TOS:3)	[233]
Bimetallic					
Pt_3Ni_{10}	CeO_2	3	723	0.0067	[17]
3Pt 10Ni	CeO_2	6	723	0.0045	
CoAl (MC)	Al_2O_3	3	823	0.144* (TOS:6h)	[176]
CoAl (M)	Al_2O_3			0.032*(TOS:6h)	
CoAl	Al_2O_3			0.136*(TOS:6h)	
CoSi (MC)	SiO_2			0.12*(TOS:6h)	

CoSi (M)	SiO_2			0.184*(TOS:6h)	
CoSi	SiO_2	3.7	973	0.168*	[234]
CuNi	SiO_2	3.7	873	0.1534	[64]
NiCe				0.37	
NiZr	SiO_2			0.62	
0.055Fe/Co	α- Al_2O_3	5	823	0.538*(TOS:3h)	[233]
Mixed Oxide					
Rh	$Ce_{0.8}Zr_{0.2}O_2$	8	723	0.011*(TOS:8.3h)	[235]
Rh	$Ce(70)Zr(30)O_2$	6	859	6.75^(TOS:20h)	[230]
Rh	$La_2O_3(15)SiO_2$	5	773	0.00003	[218]
	$La_2O_3(40)SiO_2$			0.0002	
Ni	$Ce_{0.6}Zr_{0.4}O_2$	5.8	865	0.0093	[117]
Ni	Y_2O_3-Al_2O_3(1:1)	13	773	0.033*	[215]
Cu	ZnO/ Al_2O_3	5	873	0.097*	[164]
Ni	Al_2O_3-CeO_2	3	773	0.660*	[236]
Ni	La_2O_3-Al_2O_3	4	873	0.82#	[237]
Spinel					
Ru	$MgAl_2O_4$	10	673	0.01#	[213]
Ni	$MgAl_2O_4$	10	673	0.046#	
Co	$MgAl_2O_4$	3	773	0.26	[232]
Co	$MgAl_2O_4$	4.8	923	0.302*(TOS:7h)	[204]
	$MgAl_2O_4$ with La			0.226*(TOS:7h)	
	$MgAl_2O_4$ with Pr			0.225*(TOS:7h)	
	$MgAl_2O_4$ with Ce			0.225*(TOS:7h)	
Bimetallic Spinel					
Co Pt	$MgAl_2O_4$	3	773	0.20	[232]

Co Ir	$MgAl_2O_4$			0.25	
Co Ru	$MgAl_2O_4$			0.19	
1Ag-Ni	$MgAl_2O_4$	10	673	0.41[#]	[213]
1K-Ni				0.17[#]	
Ni	$MgAl_2O_4$	6.2	865	0.028	[117]

Hydrotalcite

Co	$Mg_4Al_2(OH)_{16}]CO_3.4H_2O$	4	823	0.002	[238]
0.1 Pt	$Co_2Mg_4Al_2(OH)_{16}]CO_3.4H_2O$			0.017	
0.3Pt	$Co_2Mg_4Al_2(OH)_{16}]CO_3.4H_2O$			0.040	
0.5Pt	$Co_2Mg_4Al_2(OH)_{16}]CO_3.4H_2O$			0.031	
1 Pt	$Co_2Mg_4Al_2(OH)_{16}]CO_3.4H_2O$			0.096	
0.1Rh	$Co_2Mg_4Al_2(OH)_{16}]CO_3.4H_2O$			0.018	
0.3Rh	$Co_2Mg_4Al_2(OH)_{16}]CO_3.4H_2O$			0.012	
0.5Rh	$Co_2Mg_4Al_2(OH)_{16}]CO_3.4H_2O$			0.013	

Bimetals supported on Mixed Oxide

$Ni_{0.1}Pd$	$La_2O_3-Al_2O_3$	4	873	0.27[#]	[237]
$Ni_{0.3}Pd$				0.32[#]	
$Ni_{0.1}Pt$				0.51[#]	
$Ni_{0.3}Pt$				0.49[#]	
Pt_5Ni	$Al_2O_3-CeO_2$	3	773	0.644*(TOS:24h)	[236]
Pt10Ni				0.629*(TOS:24h)	
Pt25Ni				0.583*(TOS:24h)	
Co/Cu	ZnO/Al_2O_3	5	873	0.576*(TOS:75h)	[164]
30Ni5La	$Al_2O_3.SiO_2$	4	673	0.086	[239]

MC methanolic solution and calcined, M methanolic solution, without this aqueous solution is used. * indicates unit $g_C\,g_{cat}^{-1}$, [#] stands unit gc h^{-1}, ^ indicates unit mmol g_{cat}^{-1}, ! indicates the molar ratio of Nickel and citric acid concentration.

Research Objectives

On the basis of literature survey, it is found that among the non-noble metal catalysts cobalt and nickel in the metallic form are highly active for ESR reactions but they get deactivated due to carbonaceous deposition. The studies on unsupported Co, Ni and $NiCo_2O_4$ are missing. It was proposed in present investigation that the studies on bare metals would help to understand the mechanism of carbon formation. The catalysts deactivated by the carbonaceous deposition can be regenerated depending upon the physicochemical characteristics of used catalysts. It was also proposed that pre-treatment conditions and variation of supports may effect the activity and selectivity of catalysts for ESR reactions. The selectivity and pathways of reactions followed by Ni and Co are different and their optimal combinations may generate desired gas selectivity.

The precise objective of this thesis are as follow:

- To develop a promising non-noble metal catalyst for ESR reaction.

- To examine the sustainable approach for carbonaceous deactivation of catalyst toward making the ESR cost effective.

- To characterize the synthesized catalysts by various techniques (XRD, FTIR, surface area, SEM, XPS, TEM etc.) for their physicochemical properties.

- To evaluate the catalyst for renewable hydrogen production via ESR experimentally.

- To examine the mechanism of ESR over developed active, selective and stable non-noble catalyst.